On the Ejection of Dark Matter from Globular Clusters

T. Hurst and A. Zentner
Department of Physics and Astronomy, University of Pittsburgh, Pittsburgh, PA 15260, USA.
(Dated: February 10, 2016)

An abstract is a great convenience for the reader and is required by all journals.

PACS numbers: PACS numbers go here. These are classification codes for your research. See `http://publish.aps.org/PACS/` for more info.

I. INTRODUCTION

II. METHODS

Our calculation will follow the approach of a pair of classic papers by Hénon (Refs [1, 2] henceforth Papers 1 & 2 respectively). As in Paper 2, we begin with the assumption that the DM and stellar distributions are spherically symmetric and that the particle velocities are isotropic. Then, the number of DM particles in a volume element $\mathrm{d}^3r\mathrm{d}^3v$ is:

$$(4\pi)^2 r^2 v^2 f(r,v)\mathrm{d}r\mathrm{d}v, \tag{1}$$

where $f(r,v)$ is the DM distribution function. Similarly, if the stellar distribution function is $g(r,v',m')$ then the number of stars in the volume element $\mathrm{d}^3r\mathrm{d}^3v'\mathrm{d}m'$ is:

$$(4\pi)^2 r^2 v'^2 g(r,v',m')\mathrm{d}r\mathrm{d}v'\mathrm{d}m'. \tag{2}$$

Consider a DM particle of mass m_χ and coordinates (r,v). According to Paper 1 the probability that a particle will experience an encounter that takes it from a velocity $\vec{v} \to \vec{v} + \vec{e}$ is:

$$P = 8\pi \mathrm{G}^2 \mathrm{d}t \frac{\mathrm{d}^3 e}{e^5} \int_0^\infty m'^2\, \mathrm{d}m' \int_{v_0'}^\infty g(r,v',m') v'\, \mathrm{d}v', \tag{3}$$

where $v_0' = \frac{1}{e}|\vec{v}\cdot\vec{e} + \frac{m_\chi + m'}{2m'}e^2|$ and G is Newton's constant. As stated in §I, the one assumption of the DM particle we make is that $m_\chi \ll m'$ so

$$\begin{aligned} v_0' &= \frac{1}{e}|\vec{v}\cdot\vec{e} + \frac{e^2}{2}| \\ &= |v\cos\delta + \frac{e}{2}|. \end{aligned} \tag{4}$$

The particle will escape if

$$|\vec{v} + \vec{e}| \geq v_\mathrm{e}(r), \tag{5}$$

where $v_\mathrm{e}(r)$ is the local escape velocity. In the remainder of the paper we will denote the local escape velocity simply as v_e. Using the notation of Paper 2, let e, δ, φ be a set of spherical coordinates for the kick velocity $\vec{e}$. Then from (5) we have that,

$$v^2 + e^2 + 2ve\cos\delta \geq v_\mathrm{e}^2. \tag{6}$$

Then, assuming that the kick velocity distribution is isotropic, we can write the probability that the DM particle will esacpe in a time $\mathrm{d}t$ as:

$$Q = 8\pi \mathrm{G}^2 \mathrm{d}t \int_0^\infty m'^2\, \mathrm{d}m' \int_{v_0'}^\infty g(r,v',m') v'\, \mathrm{d}v' \int_0^{2\pi} \mathrm{d}\varphi \int \sin\delta\, \mathrm{d}\delta \int e^{-3}\, \mathrm{d}e. \tag{7}$$

For a bound DM particle it must be the case that $v < v_\mathrm{e}$, then from (6)

$$v_\mathrm{e}^2 \leq v^2 + e^2 + 2ve\cos\delta \leq v_\mathrm{e}^2 + e^2 + 2ve\cos\delta, \tag{8}$$

therefore,

$$v\cos\delta \geq \frac{-e}{2}. \tag{9}$$

Hence, we can drop the absolute value in (4). Now,

$$Q = 16\pi^2 \mathrm{G}^2 \mathrm{d}t \int_0^\infty m'^2\,\mathrm{d}m' \int_{v_0'}^\infty g(r,v',m')v'\,\mathrm{d}v' \int e^{-3}\,\mathrm{d}e \int \mathrm{d}\cos\delta, \tag{10}$$

where integration should satisfy:

$$-1 \leq \cos\delta \leq 1 \tag{11}$$

$$0 \leq e \tag{12}$$

$$v^2 + e^2 + 2ve\cos\delta \geq v_\mathrm{e}^2 \tag{13}$$

$$v\cos\delta + \frac{e}{2} \leq v' < v_\mathrm{e}. \tag{14}$$

To find the escape rate, we now integrate over the position and veolocity of the DM particle. Let N_χ be the number of DM particles in the cluster,

$$N_\chi = \int_0^\infty 4\pi r^2\,\mathrm{d}r \int_0^{v_\mathrm{e}} 4\pi v^2 f(r,v)\,\mathrm{d}v \int_0^\infty N_\chi(m)\,\mathrm{d}m, \tag{15}$$

with $f(r,v)$ normalized to 1 and $N_\chi(m) = N_\chi\delta(m-m_\chi)$ assuming the halo is composed of a single DM constituent. Then the specfic escape rate is:

$$\begin{aligned}\left|\frac{1}{N_\chi}\frac{\partial N_\chi}{\partial t}\right| &= \int_0^\infty 4\pi r^2\,\mathrm{d}r \int_0^{v_\mathrm{e}} 4\pi v^2 \frac{Q}{\mathrm{d}t} f(r,v)\,\mathrm{d}v \\ &= 256\pi^4 \mathrm{G}^2 \int_0^\infty r^2\,\mathrm{d}r \int_0^{v_\mathrm{e}} v^2 f(r,v)\,\mathrm{d}v \int_0^\infty m'^2\,\mathrm{d}m' \int_{v_0'}^\infty g(r,v',m')v'\,\mathrm{d}v' \int e^{-3}\,\mathrm{d}e \int \mathrm{d}\cos\delta,\end{aligned} \tag{16}$$

with the limits in Eqs. (11-14) satisfied and where we have taken the magnitude since $\frac{\partial N_\chi}{\partial t}$ is negative. If the magnitude of the specific escape rate is greater than τ^{-1} with τ the age of the Universe, then it is a reasonable proposition that the GC could have ejected its DM halo by the present time. We normalized Eq. (15) to N_χ rather than 1 to make this point explicit.

As noted in Paper 2, this expression looks quite intractable, but the integrals in e and δ can in fact be calculated analytically. Keeping with the notation of Paper 2 let

$$S = \int e^{-3}\,\mathrm{d}e \int \mathrm{d}\cos\delta, \tag{17}$$

and let $C = \cos\delta$. From (13)

$$C \geq \frac{v_\mathrm{e}^2 - v^2 - e^2}{2ve} = C_1, \tag{18}$$

from (14)

$$C \leq \frac{v' - \frac{e}{2}}{v} = C_2, \tag{19}$$

and from (11)

$$C_3 = -1 \leq C \leq 1 = C_4. \tag{20}$$

In order for S to be non-zero we must have that $C_1 < C_4, C_1 < C_2, C_3 < C_4$, and $C_3 < C_2$. Now $C_3 < C_4$ trivially. $C_1 < C_4$ requires that,

$$e > v_\mathrm{e} - v = e_1, \tag{21}$$

which is stronger than (12). $C_1 < C_2$ requires that,

$$e > \frac{v_\mathrm{e}^2 - v^2}{2v'} = e_2, \tag{22}$$

which is again stronger than (12). And $C_3 < C_2$ requires that,

$$e < 2(v' + v) = e_3, \tag{23}$$

which further restricts (12). C_3 will be the lower limit of the $\mathrm{d}C$ integral when $C_1 < C_3$ or when

$$e > v + v_\mathrm{e} = e_4, \tag{24}$$

and C_2 will be the upper limit when $C_2 < C_4$ or when

$$e > 2(v' - v) = e_5. \tag{25}$$

Thus, in order to determine the limits of the integrals in S, we must consider the order of e_1, e_2, e_3, e_4, and e_5. Elementary calculations show that

$$\begin{aligned} v' &\geq \frac{1}{2}(v_\mathrm{e} - 3v) = v_1' \Rightarrow e_1 \leq e_3 \\ v' &\geq \frac{1}{2}(v_\mathrm{e} - v) = v_2' \Rightarrow e_2 \leq e_3, e_2 \leq e_4, e_4 \leq e_3 \\ v' &\geq \frac{1}{2}(v_\mathrm{e} + v) = v_3' \Rightarrow e_2 \leq e_1, e_1 \leq e_5, e_2 \leq e_5 \\ v' &\geq \frac{1}{2}(v_\mathrm{e} + 3v) = v_4' \Rightarrow e_4 \leq e_5 \end{aligned} \tag{26}$$

and it is always true that $e_1 \leq e_4$ and $e_5 \leq e_3$. These relations divide the v-v' plane into 5 regions A, B, C, D, and E (see Fig. 1). In region A,

$$e_5 \leq e_1 \leq e_2 \leq e_4 \leq e_3. \tag{27}$$

Thus in region A we have,

$$\begin{aligned} S_\mathrm{A} &= \int_{e_2}^{e_4} e^{-3}\,\mathrm{d}e \int_{C_1}^{C_2} \mathrm{d}C + \int_{e_4}^{e_3} e^{-3}\,\mathrm{d}e \int_{C_3}^{C_2} \mathrm{d}C \\ &= \frac{2v'^3}{3v(v_\mathrm{e}^2 - v^2)^2} + \frac{1}{8v(v' + v)} - \frac{2v_\mathrm{e} + v}{6v(v_\mathrm{e} + v)^2}. \end{aligned} \tag{28}$$

In region B,

$$e_2 \leq e_1 \leq e_5 \leq e_4 \leq e_3. \tag{29}$$

Hence,

$$\begin{aligned} S_\mathrm{B} &= \int_{e_1}^{e_5} e^{-3}\,\mathrm{d}e \int_{C_1}^{C_4} \mathrm{d}C + \int_{e_5}^{e_4} e^{-3}\,\mathrm{d}e \int_{C_1}^{C_2} \mathrm{d}C + \int_{e_4}^{e_3} e^{-3}\,\mathrm{d}e \int_{C_3}^{C_2} \mathrm{d}C \\ &= \frac{3v_\mathrm{e}^2 - v^2}{3(v_\mathrm{e} - v)^2(v_\mathrm{e} + v)^2} - \frac{1}{4(v'^2 - v^2)}. \end{aligned} \tag{30}$$

In region C,

$$e_2 \leq e_1 \leq e_4 \leq e_5 \leq e_3. \tag{31}$$

Hence,

$$\begin{aligned} S_{\rm C} &= \int_{e_1}^{e_4} e^{-3}\,{\rm d}e \int_{C_1}^{C_4} {\rm d}C + \int_{e_4}^{e_5} e^{-3}\,{\rm d}e \int_{C_3}^{C_4} {\rm d}C + \int_{e_5}^{e_3} e^{-3}\,{\rm d}e \int_{C_3}^{C_2} {\rm d}C \\ &= \frac{3v_{\rm e}^2 - v^2}{3(v_{\rm e}-v)^2(v_{\rm e}+v)^2} - \frac{1}{4(v'^2 - v^2)} \\ &= S_{\rm B}. \end{aligned} \tag{32}$$

In region D,

$$e_5 \le e_3 \le e_1 \le e_4 \le e_2. \tag{33}$$

Here we can not simultaneously satisfy $e > e_1, e > e_2$, and $e < e_3$, thus region D is forbidden. In region E,

$$e_5 \le e_1 \le e_3 \le e_4 \le e_2. \tag{34}$$

So region E is forbidden for the same reason as D. Then Eq. (16) becomes,

$$\begin{aligned} \left|\frac{1}{N_\chi}\frac{\partial N_\chi}{\partial t}\right| = 256\pi^4 {\rm G}^2 \int_0^\infty r^2\,{\rm d}r \int_0^\infty m'^2\,{\rm d}m' \times \Bigg\{ & \int_0^{v_{\rm e}} v^2 f(r,v)\,{\rm d}v \int_{v_2'}^{v_3'} v' S_{\rm A} g(r,v',m')\,{\rm d}v' \\ & + \int_0^{v_{\rm e}/3} v^2 f(r,v)\,{\rm d}v \int_{v_3'}^{v_4'} v' S_{\rm B} g(r,v',m')\,{\rm d}v' \\ & + \int_{v_{\rm e}/3}^{v_{\rm e}} v^2 f(r,v)\,{\rm d}v \int_{v_3'}^{v_{\rm e}} v' S_{\rm B} g(r,v',m')\,{\rm d}v' \\ & + \int_0^{v_{\rm e}/3} v^2 f(r,v)\,{\rm d}v \int_{v_4'}^{v_{\rm e}} v' S_{\rm B} g(r,v',m')\,{\rm d}v' \Bigg\}. \end{aligned} \tag{35}$$

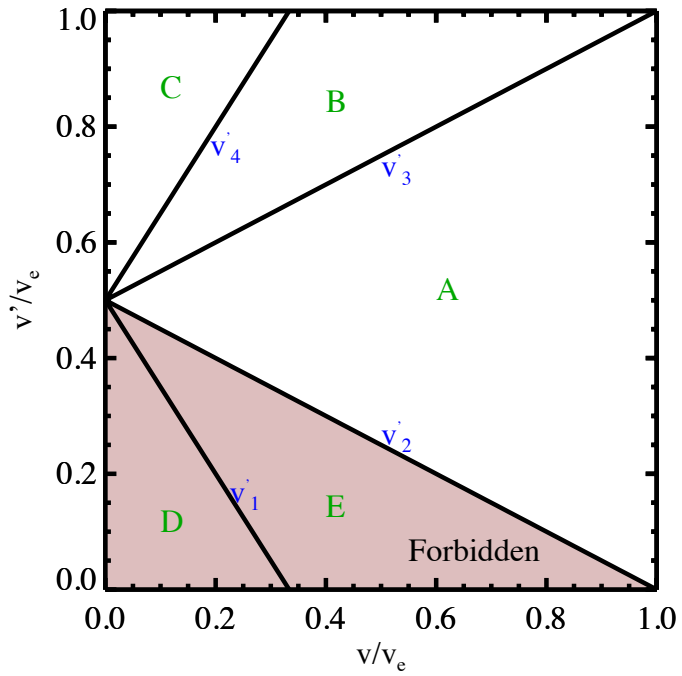

FIG. 1: The integration regions over the kick velocity $\vec{e}$. The shading denotes the fact that regions D & E are forbidden because we cannot simultaneously satisfy all of the required inequalities in Eqs. (11-14).

In order to proceed further we must specify the stellar and DM distribution functions. As in Paper 2, we take for the stellar component a Plummer model

$$\rho_*(r) = \frac{3M_*}{4\pi}\frac{r_0^2}{(r^2+r_0^2)^{5/2}}, \tag{36}$$

where r_0 is the half-mass radius of the GC. As there is little guidance on what the distribution function of DM in a GC might be, we will also use a Plummer model for the DM

$$\rho_\chi(r) = \frac{3M_{\rm DM}}{4\pi}\frac{r_\chi^2}{(r^2+r_\chi^2)^{5/2}}, \tag{37}$$

where r_χ is the half-mass radius of the DM halo. We choose the Plummer model for the DM in part because it has some nice mathematical properties that make it a convenient choice. As we shall see below, the Plummer distribution function allows us to separate the radial and velocity integrals. There is also a factor of $\left(\frac{v_{\rm e}^2-v^2}{2}\right)^{7/2}$ in the distribution function which cancels out the divergence of $(v_{\rm e}^2-v^2)^{-2}$ in $S_{\rm A}$.

Now the gravitational potential is

$$\phi(r) = \frac{-GM_*}{\left(r^2+r_0^2\right)^{1/2}} + \frac{-GM_{\rm DM}}{\left(r^2+r_\chi^2\right)^{1/2}}. \tag{38}$$

In general the half-mass radii of the 2 components need not be the same. If $r_\chi \neq r_0$ the analytic expressions needed to derive the distribution function become cumbersome and we treat this case numerically (see Fig. 2). In the case that $r_0 = r_\chi$ we will have the standard Plummer distribution

$$f(r,v) = \frac{24\sqrt{2}}{7\pi^3 r_0^3\psi_0^5}\left(\frac{v_{\rm e}^2-v^2}{2}\right)^{\frac{7}{2}} \tag{39}$$

where $\psi_0 = \frac{GM}{r_0}$ with $M = M_* + M_{\rm DM}$ the total mass of the cluster and $E = \frac{-3\pi\psi_0^2 r_0}{64{\rm G}}$ its energy.

With the choice that $r_\chi = r_0$ we have that

$$\begin{aligned} v_{\rm e} &= \sqrt{2\psi} \\ &= \frac{(2\psi_0)^{1/2}}{\left(1+\frac{r^2}{r_0^2}\right)^{1/4}}, \end{aligned} \tag{40}$$

where we have defined $\psi(r) = -\phi(r)$. Defining the stellar mass spectrum $N_*(m){\rm d}m$ as the number of stars in the mass interval $m \to m + {\rm d}m$, we have that $g(r,v',m') = f(r,v')N_*(m')$. Then Eq. 35 becomes

$$\begin{aligned} \left|\frac{1}{N_\chi}\frac{\partial N_\chi}{\partial t}\right| = \frac{2304{\rm G}^2}{49\pi^2 r_0^6\psi_0^{10}}\int_0^{R_{\rm vir}} r^2\,{\rm d}r\int_0^\infty N_*(m')m'^2\,{\rm d}m'\times\Bigg\{ &\int_0^{v_{\rm e}} v^2(v_{\rm e}^2-v^2)^{\frac{7}{2}}\,{\rm d}v\int_{v_2'}^{v_3'} v' S_{\rm A}(v_{\rm e}^2-v'^2)^{7/2}\,{\rm d}v' \\ &+\int_0^{v_{\rm e}/3} v^2(v_{\rm e}^2-v^2)^{\frac{7}{2}}\,{\rm d}v\int_{v_3'}^{v_4'} v' S_{\rm B}(v_{\rm e}^2-v'^2)^{7/2}\,{\rm d}v' \\ &+\int_{v_{\rm e}/3}^{v_{\rm e}} v^2(v_{\rm e}^2-v^2)^{\frac{7}{2}}\,{\rm d}v\int_{v_3'}^{v_{\rm e}} v' S_{\rm B}(v_{\rm e}^2-v'^2)^{7/2}\,{\rm d}v' \\ &+\int_0^{v_{\rm e}/3} v^2(v_{\rm e}^2-v^2)^{\frac{7}{2}}\,{\rm d}v\int_{v_4'}^{v_{\rm e}} v' S_{\rm B}(v_{\rm e}^2-v'^2)^{7/2}\,{\rm d}v'\Bigg\}. \end{aligned} \tag{41}$$

where the virial radius $R_{\rm vir}$ of the DM halo is chosen to be suitably large ($\sim 10r_0$)such that the integrals in Eq. (41) are all converged.

Continuing the approach of Paper 2, we now define new variables:

$$x = v/v_{\rm e}, \qquad x' = v'/v_{\rm e}. \tag{42}$$

Then we can remove $v_{\rm e}$ from the integrals over v and v' and perform those integrals seperately from the radial integral. It is proven in Appendix II of Paper 2 that the Plummer model is the only steady state distribution for which this

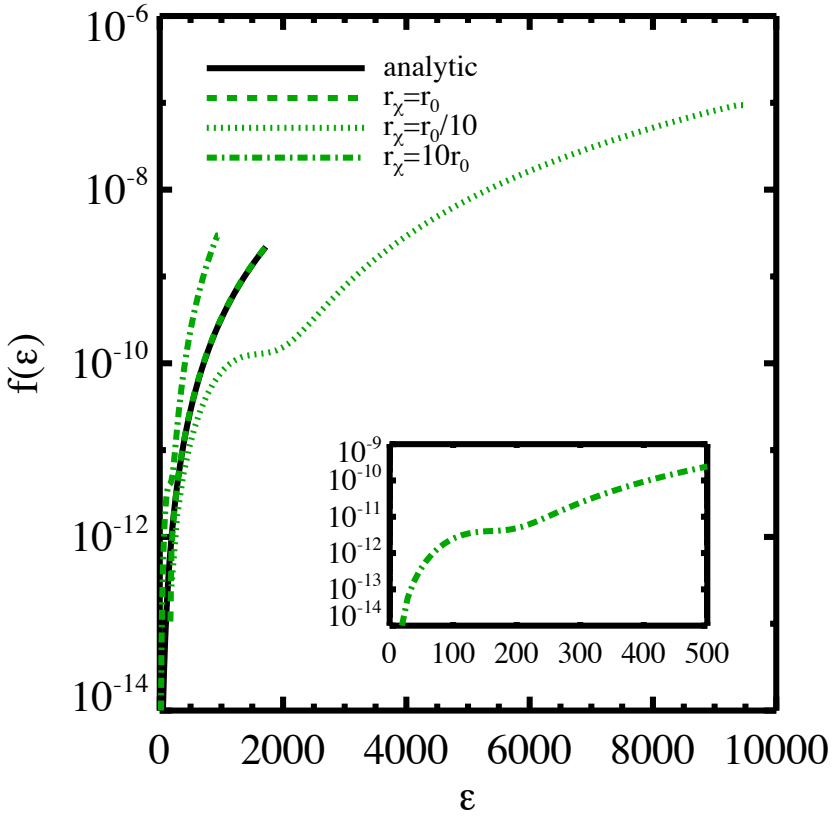

FIG. 2: The distribution function $f(\varepsilon)$ as a function of the magnitude of the specific energy $\left(\varepsilon = \frac{1}{2}[v_{\rm e}^2 - v^2]\right)$. The solid line is the standard Plummer model in the case that $r_\chi = r_0$. The dashed green line shows the numerical result for this case which is in agreement with the analytic case. The dotted line shows the distribution function in the case that $r_\chi = r_0/10$ while the dot-dashed line shows the case where $r_\chi = 10r_0$. The inset is a zoom in of the latter case, showing the feature at $\varepsilon \approx 150$.

separation is possible. Then Eq. (41) becomes

$$\begin{aligned}\left|\frac{1}{N_\chi}\frac{\partial N_\chi}{\partial t}\right| = \frac{2304\mathrm{G}^2}{49 r_0^6 \psi_0^{10}} \int_0^{R_{\rm vir}} v_{\rm e}^{17} r^2\,\mathrm{d}r \int_0^\infty N_*(m') m'^2\,\mathrm{d}m' \times \Bigg\{ &\int_0^1 x^2(1-x^2)^{\frac{7}{2}}\,\mathrm{d}x \int_{x_2'}^{x_3'} x' S'_{\rm A}(1-x'^2)^{7/2}\,\mathrm{d}x' \\ &+ \int_0^{1/3} x^2(1-x^2)^{\frac{7}{2}}\,\mathrm{d}x \int_{x_3'}^{x_4'} x' S'_{\rm B}(1-x'^2)^{7/2}\,\mathrm{d}x' \\ &+ \int_{1/3}^1 x^2(1-x^2)^{\frac{7}{2}}\,\mathrm{d}x \int_{x_3'}^1 x' S'_{\rm B}(1-x'^2)^{7/2}\,\mathrm{d}x' \\ &+ \int_0^{1/3} x^2(1-x^2)^{\frac{7}{2}}\,\mathrm{d}x \int_{x_4'}^1 x' S'_{\rm B}(1-x'^2)^{7/2}\,\mathrm{d}x' \Bigg\},\end{aligned} \tag{43}$$

where

$$\begin{aligned} x_2' &= \frac{1}{2}(1-x) \\ x_3' &= \frac{1}{2}(1+x) \\ x_4' &= \frac{1}{2}(1+3x), \end{aligned} \tag{44}$$

and the $\prime$ in S_i' denotes the fact that it is now a function of x and x' with $v_{\rm e}$ factored out.

Let us now choose a particular stellar mass spectrum. We begin with the Initial Mass Function (IMF) from Ref. [3]. All of the Galactic GCs should have ages of order ~ 10 Gyr, meaning that their Main Sequence (MS) turnoffs should be at approximately $1\,{\rm M}_\odot$. Therefore, in order to obtain a crude approximation of the present day stellar mass spectrum, we simply cut off the IMF at $1\,{\rm M}_\odot$. Note that this is highly conservative as stellar remnants such as Neutron Stars, White Dwarfs, and Black Holes as well as any stars still on the Giant and Horizontal Branches should contribute to the escape rate. Furthermore, higher mass stars are given more wait in the integral over mass in Eq. (43) (see Fig. 3).

With this choice of stellar mass spectrum we have that

$$\int_0^\infty N_*(m')m'^2\,{\rm d}m' = 0.18M. \tag{45}$$

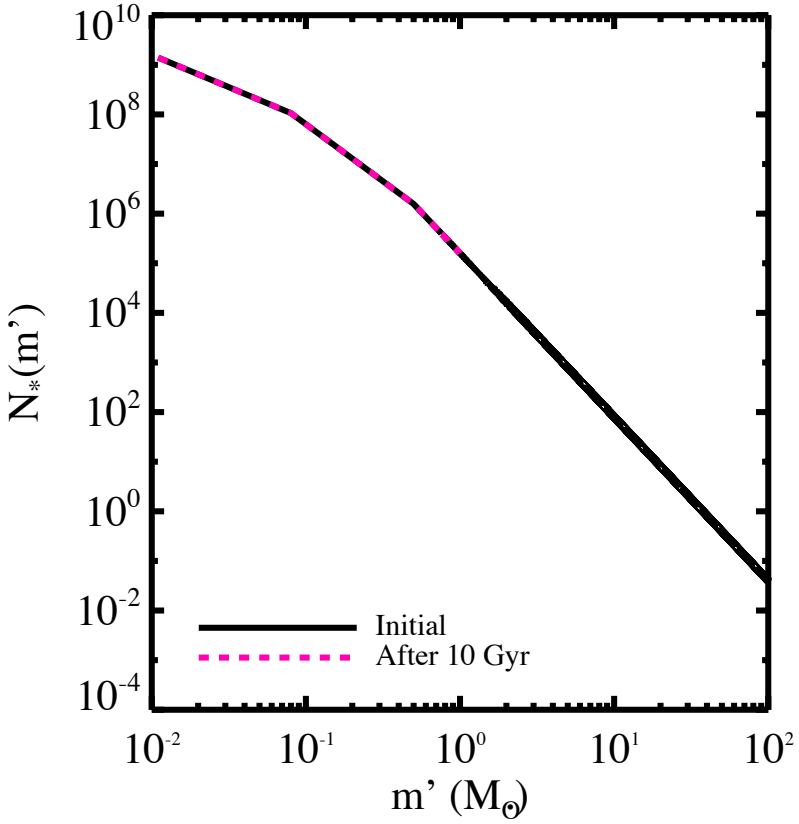

FIG. 3: The solid black line is the IMF from Ref. [3]. After 10 Gyr (the approximate age of a Galactic GC) stars more massive than $1\,{\rm M}_\odot$ will have left the MS. We therefore cut the IMF off at $1\,{\rm M}_\odot$ in order to approximate the present day stellar mass spectrum. This is a highly conservative choice as the remnants of more massive stars and stars still on the Giant and Horizontal Branches should also contribute to the escape rate.

III. RESULTS

In Fig. 4 we consider the result of integrating Eq. (43) numerically for different values of the ratio $M_{\rm DM}/M_*$ and compare these results to the Galactic GCs (as well as the cluster MGC1 located in M31). As noted in §I, most of the Galactic GCs could have lost their DM halos through tidal interactions with the Galaxy. We shall therefore pay particular attention to the most isolated GCs (galactocentric distance $R_{gc} > 70\,{\rm kpc}$). First consider the upper left panel. For large values of $M_{\rm DM}/M_*$ the escape rate is much too low for a significant portion of the halo to have been ejected. However, observations of several GCs (NGC 6397, MGC1, NGC2419) indicate that $M_{\rm DM}/M_* \lesssim 1$ [4, 5].

While NGC 6397 could have had its halo tidally stripped, MGC1 and NGC 2419 are extremely isolated (at 200 kpc away from M31, MGC1 is the most isolated cluster in the local group while NGC 2419 lies some 90 kpc from the center of the MW) and therefore orbit in weak tidal fields and should have retained their primordial DM halos [5]. Our results therefore rule out the possibility that these clusters formed with significant DM halos. The remaining panels demonstrate that regardless of the value of $M_{\rm DM}/M_*$ GCs cannot have ejected a significant amount of DM by multi-body interactions. Note that the escape rate is no longer sensitive to the value of $M_{\rm DM}/M_*$ once this ratio has dropped below $\approx 10^{-2}$.

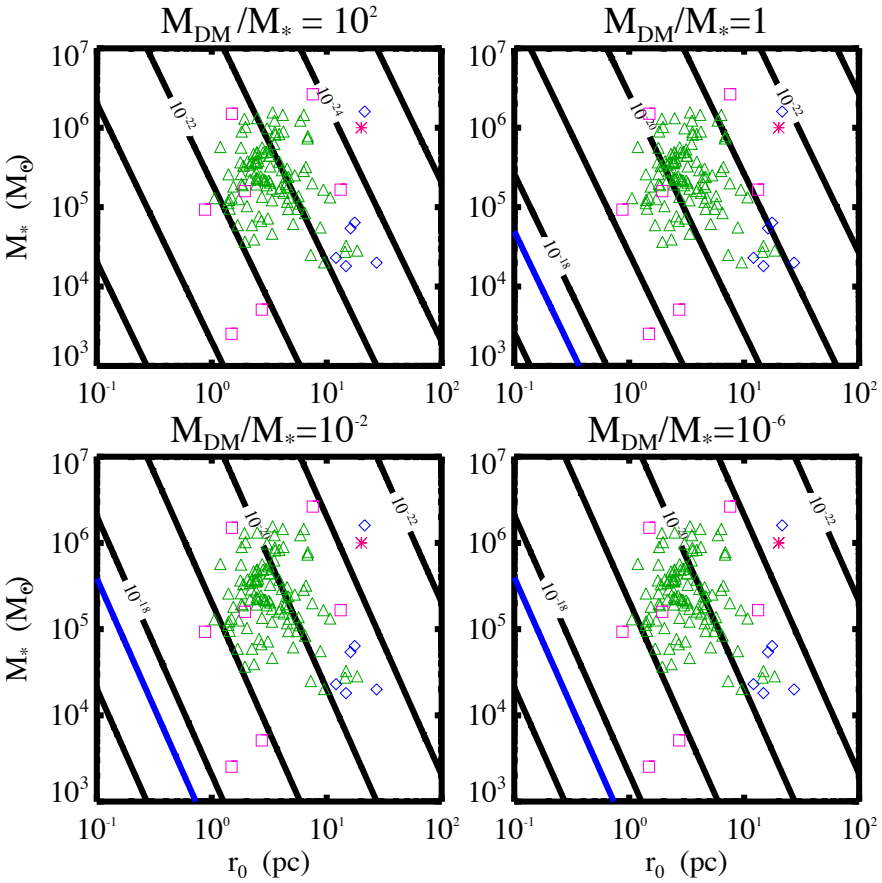

FIG. 4: Contours of the specific escape rate for GCs with $r_0 = r_\chi$. Each panel shows a different value of the ratio $M_{\rm DM}/M_*$. The red star represents MGC1, an isolated cluster orbiting M31, while the blue diamonds represent the isolated popluation of Galactic GCs ($R_{gc} > 70$ kpc). These isolated GCs are further considered in Fig. 6. Galactic GCs that have been selected for further investigation in Fig. 5 are marked with pink squares while the green triangles denote the remaining Galactic GCs. The solid blue line is the location where the specific escape rate is $1/\tau$ with $\tau = 13.8$ Gyr the approximate age of the Universe [6, 7]. GCs with escape rates comparable to or exceeding this limit should have ejected a significant portion of their DM halos. However, none of the clusters reach this limit regardless of the value of $M_{\rm DM}/M_*$, with the most massive halos having the lowest escape rates as expected.

In Figs. 5 & 6 we consider the effect of varying r_χ with respect to r_0 with $M_{\rm DM}/M_* = 1$. We consider $r_\chi = 10 r_0$ which might correspond to an extended primordial halo as well as $r_\chi = 10^{-1} r_0$ which might correspond to a cluster which has had the outer part of its DM halo stripped by tidal interactions. The results are obtained by integrating Eq. (35) with the appropriate numerically derived distribution functions (see Fig. 2). We first consider the GCs marked with pink squares in Fig. 4. The parameters for these clusters are summarized in Table I and span the full range of Galactic GCs. Note that decreasing (increasing) r_χ increases (decreases) the escape rate. This result is perhaps counter intuitive as a smaller (larger) halo should have a deeper (shallower) potential well which is correspondingly more (less) difficult to escape from. However, in a smaller (larger) halo, the probability of experiencing an encounter is much higher (lower), which explains the results. Note, that for $M_{\rm DM}/M_* = 1$ the only halo which exceeds $1/\tau$ is that of Pal 1 in the case that $r_\chi = 10^{-1} r_0$. However, the escape rate can be increased by an additional half dex for smaller values of the ratio $M_{\rm DM}/M_*$. Fig 5 then indicates that clusters with $M_{\rm DM}/M_* \lesssim 10^{-2}$, $M_* \lesssim 10^5\,{\rm M}_\odot$, and

GC	$M_*(\mathrm{M}_\odot)$	r_0 (pc)	$M_{\rm DM}/M_*$
Pal 1	2.54×10^3	1.49	—
Pal 13	5.12×10^3	2.72	—
NGC 5053	1.66×10^5	13.2	—
NGC 5139	2.64×10^6	7.56	—
NGC 6388	1.50×10^6	1.50	—
NGC 6397	1.59×10^5	1.94	$\lesssim 1$ [4]
NGC 6528	9.31×10^4	0.87	—

TABLE I: Parameters for the GCs marked with pink squares in Fig. 4 and selected for further consideration in Fig. 5 [8].

r_0 not more than a few parsecs, could have ejected a small remnant halo after the initial halo was tidally stripped.

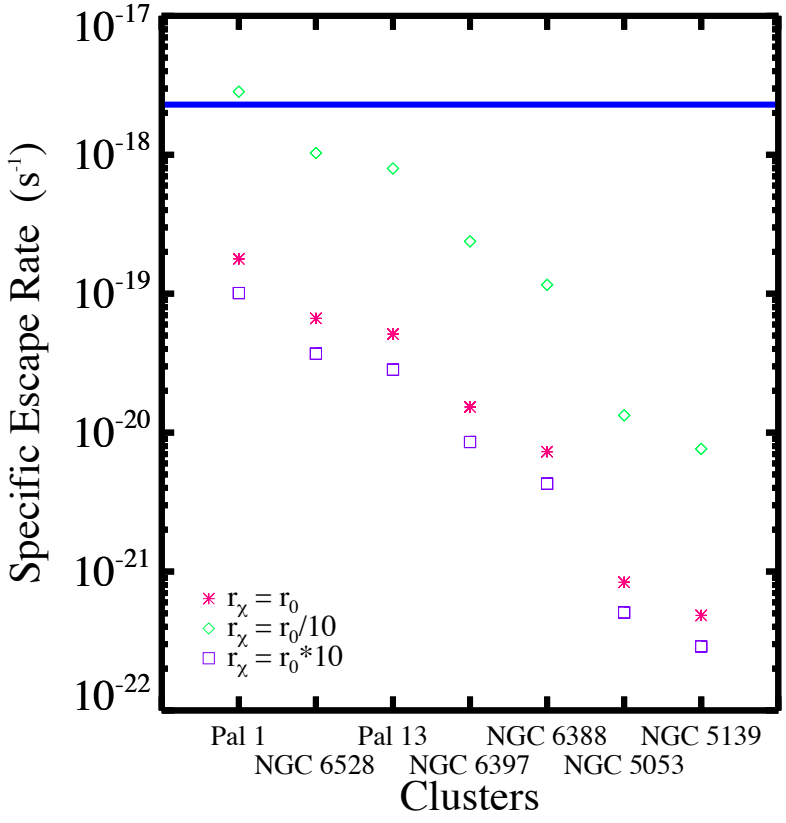

FIG. 5: Escape rates for several Galactic GCs for different values of r_χ/r_0 under the assumption that $M_{\rm DM}/M_* = 1$. The solid blue line denotes $1/\tau$.

In Fig. 6 we consider the escape rates for the most isolated clusters in the Milky Way (and M31) which are marked with blue diamonds in Fig 4. The parameters for these clusters are summarized in Table II. Due to their large sizes ($r_0 > 10\,\mathrm{pc}$) these clusters all have escape rates well below $1/\tau$. Since these clusters should not have lost their halos through tidal interactions, we conclude as in Ref. [5] that these clusters did not form in significant DM halos.

GC	$M_*(\mathrm{M}_\odot)$	r_0 (pc)	R_{gc} (kpc)	$M_{\rm DM}/M_*$
AM 1	1.81×10^4	14.7	124.6	—
Eridanus	2.30×10^4	12.1	95.0	—
Pal 3	6.38×10^4	17.5	95.7	—
Pal 4	5.41×10^4	16.1	111.2	—
NGC 2419	1.60×10^6	21.4	89.9	$\lesssim 1$ [5]
Pal 14	2.00×10^4	27.1	71.6	—
MGC1	1×10^6	20	200	$\lesssim 1$ [5]

TABLE II: Parameters for the isolated GCs marked with blue diamonds in Fig. 4 and selected for further consideration in Fig. 6 [8].

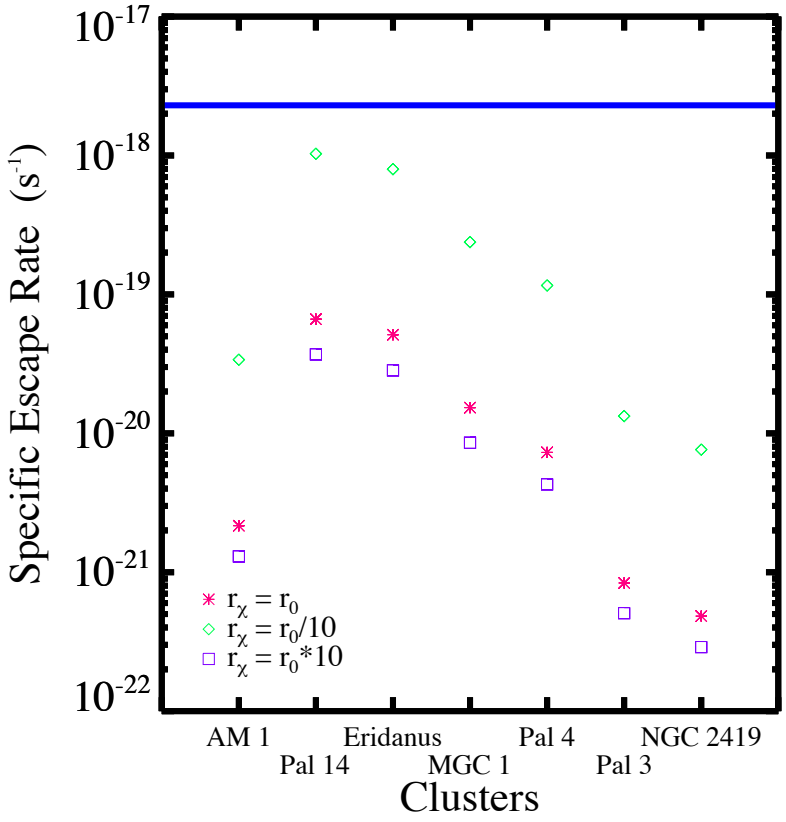

FIG. 6: Escape rates of the isolated GCs for different values of r_χ/r_0 under the assumption that $M_{\rm DM}/M_* = 1$. The solid blue line denotes $1/\tau$.

IV. CONCLUSIONS

Acknowledgments

[1] M. Hénon, Annales d'Astrophysique **23**, 467 (1960).
[2] M. Henon, Astronomy and Astrophysics **2**, 151 (1969).
[3] P. Kroupa, MNRAS **322**, 231 (2001), astro-ph/0009005.
[4] J. Shin, S. S. Kim, and Y.-W. Lee, Journal of Korean Astronomical Society **46**, 173 (2013).

[5] C. Conroy, A. Loeb, and D. N. Spergel, Astrophys. J. **741**, 72 (2011), 1010.5783.
[6] G. Hinshaw, D. Larson, E. Komatsu, and *et al.*, APJS **208**, 19 (2013), 1212.5226.
[7] P. Collaboration (????).
[8] W. E. Harris, The Astronomical Journal **112**, 1487 (1996).